HyDesign: a tool for sizing optimization for grid-connected hybrid power plants including wind, solar photovoltaic, and Li-ion batteries

Juan Pablo Murcia Leon[1], Hajar Habbou[1], Mikkel Friis-Møller[1], Megha Gupta[1], Rujie Zhu[1], and Kaushik Das[1]

[1]Department of Wind and Energy Systems, Technical University of Denmark, 4000 Roskilde, Denmark

Correspondence: Juan Pablo Murcia (jumu@dtu.dk)

Abstract. Hybrid renewable power plants consisting of collocated wind, solar photo-voltaic (PV) and Lithium-ion battery storage connected behind a single grid connection can provide additional value to the owners and to society in comparison to individual technology plants such as only wind or only solar-PV. These benefits become significant in projects that have requirements to supply a certain amount of energy during peak hours given a set of grid capacity constraints or when the plant

5   is selling the electricity with time-varying electricity prices. The hybrid power plants considered in this article are connected to the grid and share electrical infrastructure costs across the different generation and storing technologies. In this article, we propose a methodology for sizing of hybrid power plants as an optimization problem that maximizes the net present values over capital expenditures and compares it with standard designs that minimize the levelized cost of energy. The sizing problem formulation includes turbine selection (in terms of rated power, specific power and hub height), a wind plant wake

10   losses surrogate, simplified photo-voltaic panel degradation, an internal energy management system operation optimization and battery degradation. The multi-disciplinary optimization problem is solved using a new parallel "efficient global optimization" algorithm. This new algorithm is a surrogate-based optimization method that ensures a minimal number of model evaluations but ensures a global scope in the optimization. The methodology presented in this article is available in an open-source tool called HyDesign. The hybrid sizing algorithm is applied for a peak-power plant use case at different locations in India where

15   the renewable energy auctions impose a monetary penalty when energy is not supplied at peak hours.

1 Introduction

Hybrid power plants (HPP) consisting of collocated wind, solar photo-voltaic (PV) and Lithium-ion battery storage connected behind a single grid connection point can provide better returns of investment than individual source (wind or solar) plants in locations where the wind and solar resources are comparable and for electricity markets in which fixed power purchase

20   agreement electricity prices are not possible. HPP can be designed to have operational flexibility in terms of dispatchability and ancillary service provision that makes them closer to traditional power plants in terms of achieving additional profitability in markets with time-varying electricity prices under grid connection constraints and that have reduced costs due to the shared infrastructure (Gorman et al., 2020; Dykes et al., 2020).

Sizing of HPP plant is a multi-discipline analysis and optimization (MDAO) problem that requires detailed modeling of the wind and solar resources as well as the wind, PV and storage performance, costs and operation (Dykes et al., 2020). Additionally, the selection of the wind turbine characteristics (specific power, hub height) and PV characteristics (panel orientation) are additional degrees of freedom that can significantly modify the results of the sizing. Traditional objective functions of the sizing optimization problem are maximizing net annual energy production or minimizing levelized cost of energy (LCoE) (Tripp et al., 2022), but in general HPP designs that include energy storage can produce more revenues relative to the cost increase. In this article, we compare HPP sizing optimization for both LCoE and relative net revenues as objective functions.

A detailed energy management system (EMS) is required to determine the operation of the battery given the time-series of wind and solar generation and the battery's capacity. EMS optimization will determine when to charge and discharge the battery with the objective of maximizing the revenue obtained by the HPP. Several articles focus on formulating EMS optimization problems and propose different formulations Al-Lawati et al. (2021); Das et al. (2020); Khaloie et al. (2021a, b); Wang et al. (2019). Different levels of complexity can be studied in the implementation of EMS such as: (1) rule-base algorithms that prescribe the operation of the battery, (2) deterministic EMS optimization that maximizes the revenues assuming perfect forecasts (full future-knowledge) on the price of electricity, the wind and solar generation time-series, (3) robust optimization of EMS operation will provide battery operation under worst case scenarios of forecast errors of generation and prices time-series, and (4) Stochastic optimization of EMS operation that will provide best operation over the entire distribution of forecasting error. EMS operational optimization within the HPP sizing optimization is not common in the literature but it is required in order to unravel the value of hybrid plants fully.

Furthermore, HPP sizing requires solving the long-term performance of the different components through the lifetime of the HPP project; this implies modeling the degradation in the performance of the individual components. Li-ion batteries and PV cells have significant degradation over time, several models of degradation exist (Jordan et al., 2016), while wind turbine is assumed not to have significant performance degradation since the internal wind turbine pitch control system will ensure that the rated power and performance of the turbine is kept approximately constant over its lifetime.

Typically, battery cells have to be replaced when their capacity degrades beyond a pre-defined threshold. The higher CAPEX of new batteries plays a dominant role in battery operation cost, i.e. degradation cost. Therefore, considering battery degradation when sizing HPP can optimize the use of battery and hence extend battery lifetime and reduce costs. Battery degradation is a complicated chemical process. Theoretical studies (Safari et al., 2008; Vetter et al., 2005) on battery degradation explains the detailed degradation mechanism of battery cells. However, the required parameters and conditions of the battery cell can not be obtained in the sizing stage. To incorporate the battery degradation model into the sizing problem, it is possible to use semi-empirical models (Xu et al., 2016) that only require the state of charge time-series (SoC) as input to assess battery lifetime. This model considers the solid electrolyte inter-phase film formation theory calibrated based on experimental observations and it is able to describe the non-linear degradation process.

To the authors' knowledge, there is no available sizing methodology for the design of utility-scale grid-constrained hybrid power plants considering all the above-mentioned characteristics. This article presents a general methodology for hybrid plant sizing as a MDAO including several novel aspects: (1) turbine selection (2) PV degradation (3) battery degradation (4) internal

EMS operation optimization. We apply the methodology and report the detailed result of the hybrid plant design in three
60   different locations in India: (a) solar dominant site (b) wind dominant site and (c) low wind and solar resources.

India is a large market in which hybrid plants could become important because of the need to provide renewable energy that
supports the demand patterns and because of the intermediate solar and wind resources. For this reason, Indian sites are used
as example cases in this article.

2   Methodology

65   The design of a HPP is an optimization problem that involves several sub-optimization problems such as: wind turbine se-
lection, siting and layout optimization, PV array sitting, energy management system (EMS) operation optimization coupled
with battery degradation and electrical infrastructure optimization. Early HPP sizing optimization focused on maximizing the
viability of a HPP installation in a given location requires a simplified approach. The XDSM diagram of the HPP sizing opti-
mization problem is presented in figure 1. In the sizing optimization several simplifications are performed in order to reduce the
70   complexity of the optimization: (1) the WT Layout optimization is replaced by a surrogate of the wakes of sub-optimal wind
turbine layouts, (2) uncoupled battery and PV degradation models reduce the complexity of the EMS optimization, a short-term
EMS optimization problems is proposed that considers a constrain in battery utilization, while a long-term operation rule-based
EMS corrects the ideal operation for degradation, (3) approximate electrical infrastructure costs are used.
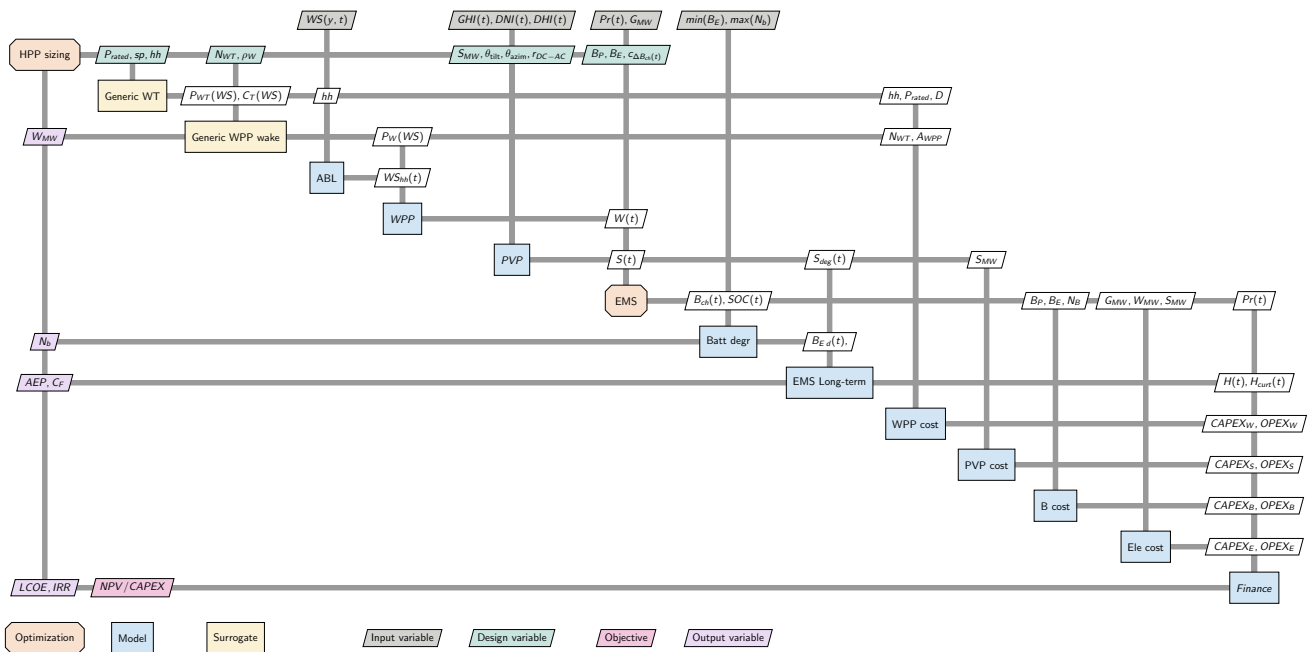
Figure 1. HPP sizing XDSM diagram.

2.1 Generic Wind Turbine

75 A look-up table is built based on DTU's pywake generic turbine model (Pedersen et al., 2023). The interpolation of this data is a surrogate that predicts the power and thrust coefficient curves given the turbine's specific power, defined as the ratio between the rated power and the rotor area ($sp = P_{rated}/A$). The wind turbine power curve and thrust coefficient curves are represented as $P_{WT}(\text{WS})$ and $C_T(\text{WS})$ in figure 1. Examples of the surrogate power and thrust coefficient curves are given in figure 2.
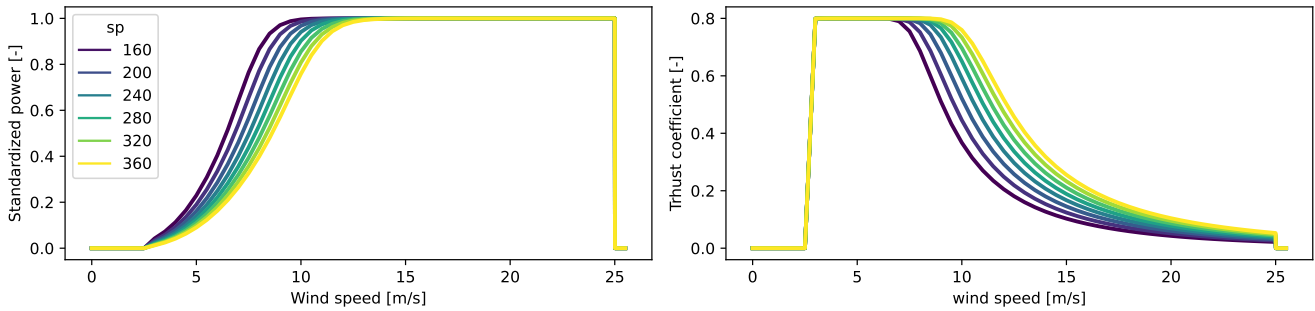
Figure 2. Generic Wind Turbine surrogate.

2.2 Generic Wind Power Plant Wake Model

80 A database of wind power plants is generated using circular plant borders and a simplified layout optimization that maximizes the distance between the turbines. Two example layouts are presented in figure 3. Wakes are simulated using *pyWake*'s implementation of Zong's wake model (Pedersen et al., 2023; Zong and Porté-Agel, 2020) which combines a Gaussian wind speed deficit with local turbulence dependent linear wake expansion, with squared sum wake deficit superposition model and Frandsen's added turbulence model as specified in the IEC wind turbine design standard (Commission et al., 2017).

85 Detailed wake losses as a function of wind speed and wind direction are simulated for multiple WPP layouts with the same number of turbines and installation density (ρ_W, plant-rated power over the land use area, [MW/km^2]) for a given turbine's specific power. The results are aggregated taking the 90-th larger quantile wake losses across wind directions and across 20 layouts generated using a different random seed number. A surrogate of the wake losses curve (WL(WS)) is built as a function of the installation density, number of turbines and specific power of the turbine. Example results of the surrogate are presented

90 in Figure 4. Finally, the generic wind plant model will combine the turbine power curve with the expected wake losses to provide a wake-affected plant power curve, see equation 1.

$$\text{WL}(\text{WS}) \approx \hat{\text{WL}}(N_{WT}, sp, \rho_W, \text{WS})$$
$$P_W(\text{WS}) = P_{WT}(\text{WS}) * (1 - \text{WL}(\text{WS}))$$

(1)
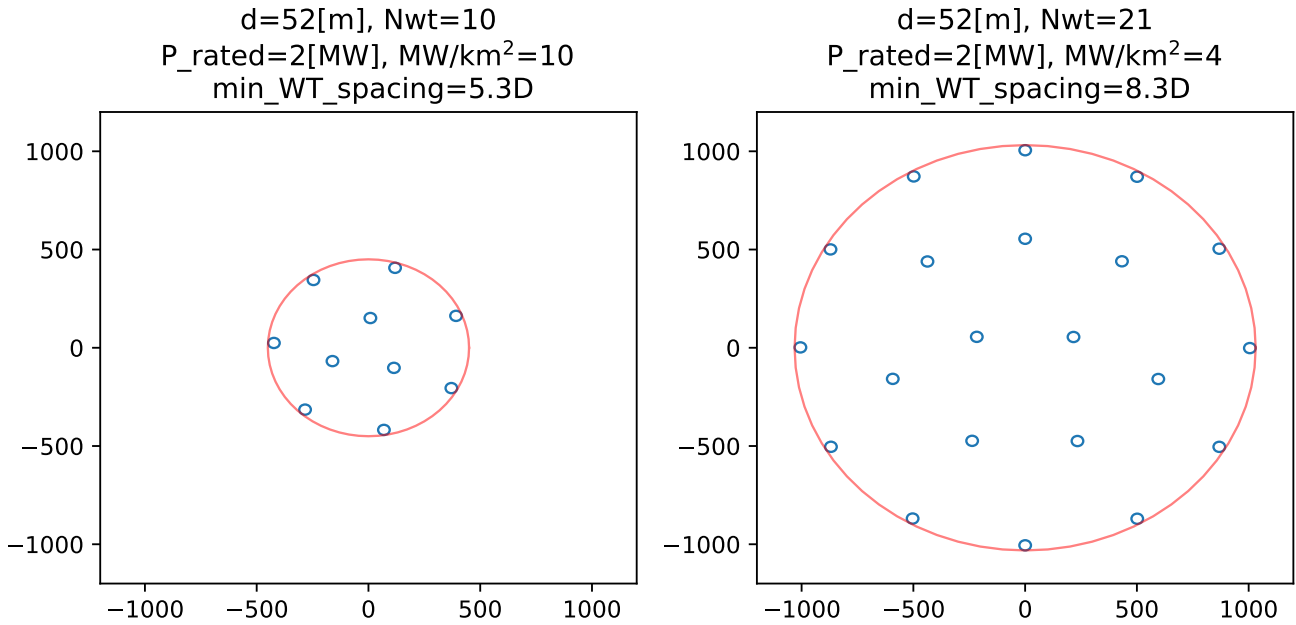
Figure 3. WPP example of generated layouts.
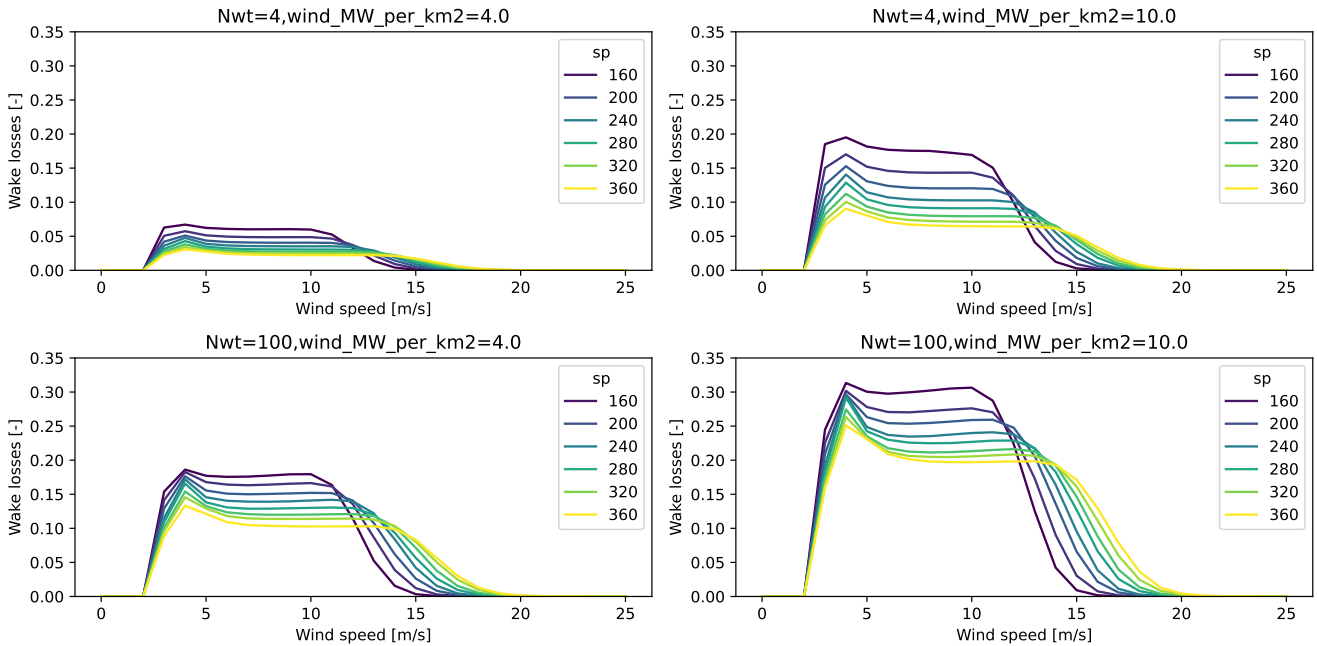
Figure 4. Example wake losses as a function of the number of turbines, installation density [MW/km^2] and turbine's specific power.

2.3 Weather

ERA5 (Hersbach et al., 2020) is used as a reanalysis dataset for wind resource calculations. The hourly wind velocity time-series with a 0.25x0.25 degree resolution in latitude and longitude are interpolated into heights of 50, 100, 150 and 200 [m]. This dataset is stored and interpolated at the location of hybrid power plant using linear interpolation in the horizontal coordinates, keeping the hub height dimension of the velocities in order to compute the effect of changing the hub height of the turbines in the optimization.

The mean wind speed from the Global Wind Atlas 2 (GWA2) is used for correcting ERA5's mean wind speed following the approach presented in (Murcia et al., 2022). This scaling correction is necessary in order to include the first order effects of terrain. The corrected wind speed time-series is provided on multiple heights ($\mathrm{WS}(y,t)$) to the atmospheric boundary layer (ABL) model. This model uses a piece-wise power law interpolation to determine the wind speed time-series at hub height ($\mathrm{WS}_{hh}(t)$).

ERA5-land is used as a reanalysis of the hourly global horizontal irradiance time-series ($\mathrm{GHI}(t)$) because it has a better resolution than ERA5, 0.1 degrees versus 0.25 degrees in latitude and longitude resolution, and it shows a better validation metrics for individual plant modeling (Camargo and Schmidt, 2020). Decomposition of GHI to direct normal irradiance (DNI) and diffuse horizontal irradiance (DHI) is done in two steps: the DISC model is used to estimate the DNI (Maxwell, 1987) using the GHI and relative air mass model based (Kasten and Young, 1989). While the DHI is estimated using the solar position, see equation 2.

$$\mathrm{DHI}(t) = \mathrm{GHI}(t) - \mathrm{DNI}(t) * \cos(\theta_{\mathrm{zenith}}(t)) \tag{2}$$

2.4 Wind power plant model (WPP)

The wind generation time-series ($W(t)$) is obtained by interpolating the plant power curve at the hub height's wind speed time-series, scaling the generation by the installed capacity. Additionally, an efficiency ($\eta_W = 0.95$) is assumed to cover the electrical and availability losses, see equation 3.

$$W(t) = N_{WT} * P_{rated} * P_W(\mathrm{WS}_{hh}(t)) * \eta_W \tag{3}$$

2.5 PV power plant model (PVP)

Power conversion uses PVLib (Holmgren et al., 2018) based on a generic 1MW PV plant configuration (PV module, inverter and open rack with glass-glass) with the irradiance projection transposition model (Davies and Hay, 1978), the Sandia array performance model (SAPM) (King et al., 2004) and Sandia performance model for grid-connected PV-inverter model (King et al., 2007). The final solar PV generation requires the plant capacity, the orientation of the panels in terms of tilt and azimuth angles ($\theta_{\mathrm{tilt}}, \theta_{\mathrm{azim}}$), the ratio between DC and AC sides of the inverter ($C_{S\,inverter}$), the irradiances (DNI, DHI), the wind speed close to ground ($\mathrm{WS}_1(t)$) and the ambient temperature ($T_1(t)$), see equation 4.

$$S(t) = S_{MW} * \text{PV}(\theta_{\text{tilt}}, \theta_{\text{azim}}, r_{DC-AC}, \text{DNI}(t), \text{DHI}(t), \text{WS}_1(t), T_1(t)) \tag{4}$$

The PV degradation model is a linear loss of capacity lost over the lifetime given a degradation per year (default value of
125 0.5% per year).

2.6 Electricity price

The electricity price time-series in the Spot market ($Pr(t)$) is an input to the model, note that the price time-series need to be correlated with the weather time-series. This report focuses on valuation of time varying power purchase agreements as the ones that have been seen in the Indian HPP market. This price signals has two levels of electricity price at peak and non-peak
130 (demand) hours. An example of the peak non-peak PPA electricity price is presented in figure 5.

2.7 Energy management system optimization model (EMS)

The energy management system optimization model consists in selecting the amount of battery charge/discharge and power curtailment that maximizes the revenue generated by the plant over a period of time (usually one or two years), including a possible penalty for not meeting the requirement of energy generation and a penalty for battery power ramping to control
135 the amount of battery degradation, see equation 5. Note that the EMS optimization is solved using linear programming and therefore does not compute the battery degradation, instead, it assumes new battery and PV panels (without degradation). The idealized EMS operation design also assumes perfect knowledge of both the weather and price, and therefore there are neither forecasting errors on the prices nor weather.

The revenue is given by the product of electricity price ($Pr(t)$) and the HPP power generation ($H(t)$) minus the penalty over
140 the period (l) and minus the battery ramping penalty (l_b). The HPP generation is defined as the total power from wind ($W(t)$), solar PV ($S(t)$), battery charge or discharge ($B(t)$) and power curtailment ($P_{curt}(t)$).

The penalty (l) is the missing energy generated at peak times with respect to the energy requirement over the period (E_l) times a mean peak electricity price ($\overline{Pr(t_{peak})}$). The penalty can only be positive, which means that it can only subtract revenue, and not give extra revenue to generate above the requirements.

145 The battery fluctuations penalty (l_b) is defined as the sum of the products of the absolute battery power fluctuations ($|\Delta B(t)|$) and the difference between max electricity price and the current price ($Pr_{max} - Pr(t)$). This means that large fluctuations in the battery charge/discharge are allowed when the price is high. The battery fluctuation penalty factor (C_{bfl}) is a design variable that captures how strongly can the battery be ramped and therefore it controls the battery degradation, when C_{bfl} is 0 then large changes in charge/discharge occur, see figure 5.

150 The constraints in the optimization keep track of battery level ($E_{SOC}(t)$), enforcing the batteries energy ($B_E(t)$) and power capacity (B_P), force the grid constraints, including an asymmetric charging/discharging efficiency ($\eta_{charge}, \eta_{discharge}$), a minimum level of battery discharge ($B_{E\,depth}$).

$$\max \quad \sum_t \left(Pr(t) \times H(t) \right) - l - l_b$$

$$\text{with} \quad l = \begin{cases} E_l \times \overline{Pr(t_{peak})} & \text{if} \quad E_l > 0 \\ 0 & \text{if} \quad E_l \le 0 \end{cases}$$

$$E_l = \left(E_{peak\,req} - \sum_{t \in t_{peak}} (H(t)\,\Delta t) \right)$$

$$l_b = C_{bfl} \times \sum_t |\Delta B(t)| \times [Pr_{max} - Pr(t)]$$

$$\text{such that } \forall t \quad H(t) = W(t) + S(t) + B(t) - P_{curt}(t) \tag{5}$$

$$H(t) \le G$$

$$E_{SOC}(t+1) = \begin{cases} E_{SOC}(t) - \eta_{charge} B(t)\,\Delta t & \text{if} \quad B(t) \le 0 \\ E_{SOC}(t) - B(t)\,\Delta t / \eta_{discharge} & \text{if} \quad B(t) \ge 0 \end{cases}$$

$$E_{SOC}(t) \ge B_E(t) \times [1 - B_{E\,depth}]$$

$$E_{SOC}(t) \le B_E(t)$$

$$B(t) \le B_P$$

$$B(t) \ge -B_P$$
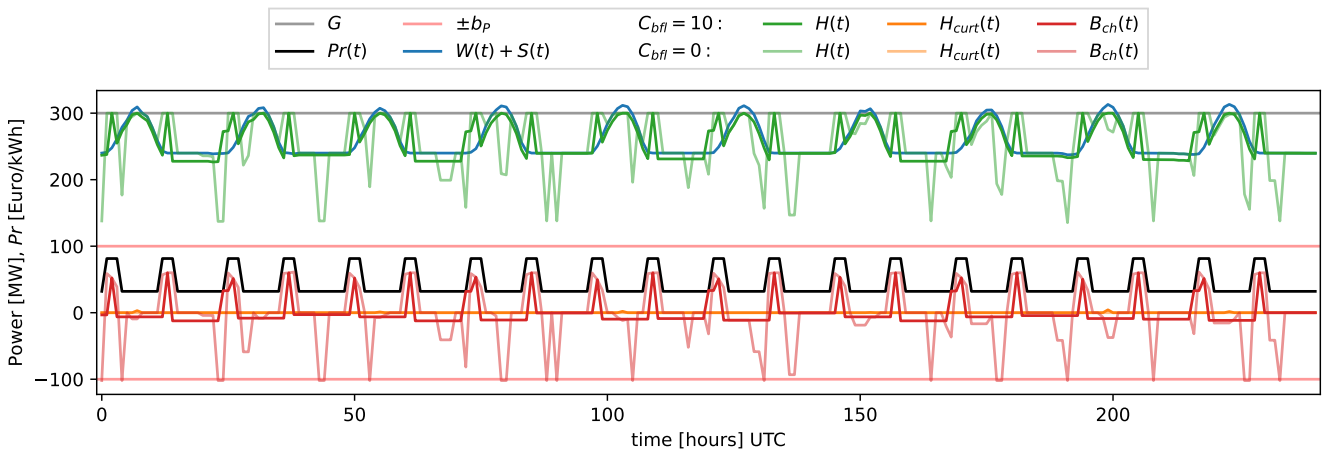
Figure 5. EMS comparison in an example HPP for two different battery fluctuation penalty factor C_{bfl}.

2.8 Battery degradation model

155 The battery degradation model includes the linear degradation rate regarding cycle numbers and the non-linear degradation due to the solid electrolyte interphase film formation process in the early stage of the battery life. A rainflow counting (Downing and Socie, 1982; Shi et al., 2018) is implemented to obtain the depth of discharge (R_{DoD}), mean state of charge cycle (R_{SoC}), half or full cycle count (R_{count}), for a number of cycle frequencies (n_R) given a state of charge time-series ($E_{SOC}(t)$).

The linear degradation rate (f^d) in equation 6 depends on a stress model due to the depth of discharge ($S_{DoD}(R_{DoD})$), a
160 stress model due to cycle count and age of the battery ($S_t(R_{count}, t_c)$), a stress model due to state of charge ($S_{SoC}(R_{SoC})$), and a stress model due to cell temperature ($S_T(T_c)$). The stress factor models are empirical relationships calibrated on measurements (Xu et al., 2016).

$$f^d = \sum_{j=1}^{n_R} [S_{DoD}(R_{DoD,j}) + S_{t_c}(R_{count,j}, t_c)] \times S_{SoC}(R_{SoC,j}) S_{T_c}(T_c) \tag{6}$$

The non-linear part of the degradation given in Eq. 7 calculates the loss of storing capacity (LoC, L) using two models: fresh
165 battery and used battery after the formation of SEI film. A pre-defined LoC level is used to determine in which regime is the battery (L_1). L' and $f^{d'}$ are the LoC and linear estimation of LoC when L exceeds L_1 at the first time. Where the parameters of the model take the following values $\alpha = 0.0575$ and $\beta = 121$.

$$L = \begin{cases} 1 - \alpha \, e^{-\beta f^d} - (1-\alpha) e^{-f^d} & if \, L \leq L_1 \\ 1 - (1-L') \, e^{-f^d + f^{d'}} & if \, L > L_1 \end{cases} \tag{7}$$

Finally, the remaining energy capacity of the battery B_E, is the remaining of loss factor of the original energy storing
170 capacity: $B_E(t) = B_{E\,new} \times [1 - L(t)]$. In this article, the battery degradation model is not coupled to the EMS model, but instead it uses the resulting state of charge time-series (SoC) estimated by the EMS optimization on an operation period (for example one or two years). The SoC operation period is repeated to have a full lifetime of operation to compute the degradation over the lifetime of the HPP. The continuous degradation curve is discretized in periods of constant health levels in order to simplify the implementation of the long-term operation correction. Finally, battery replacement occurs when the battery reaches
175 a minimum health level (70%), see Figure 6.
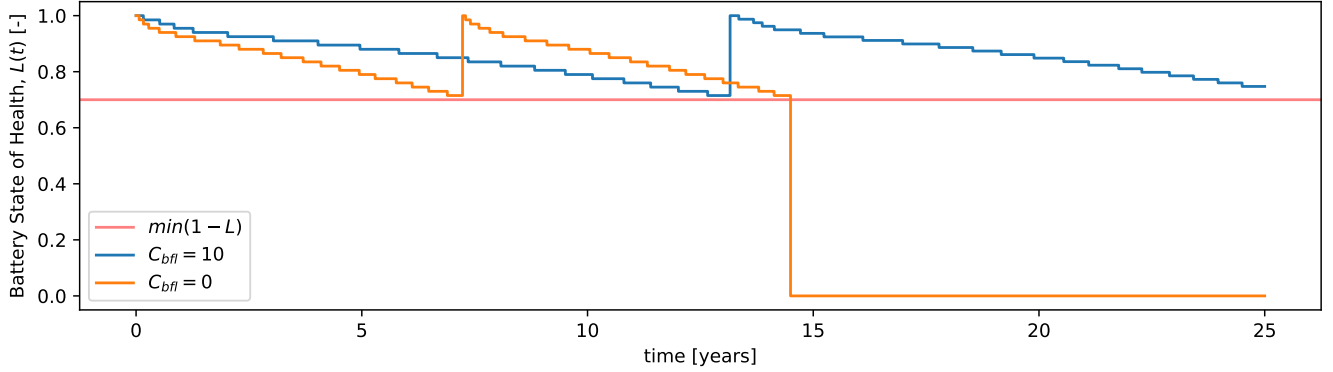
Figure 6. Battery degradation comparison in an example HPP for two different battery fluctuation penalty factor C_{bfl}.

2.9 Long-term operation: Rule-based Energy management system correction model (EMS Long-term)

A ruled based EMS is implemented in order to account for battery degradation, degradation in PV and forecast errors in estimated wind and solar generation without having to run new EMS optimizations. The correction model consists in the following general principles: (1) try to follow the ideal EMS operation if possible, (2) update the state of charge to account for
180   reduction in the available generation in the HPP and the new limits of the degraded battery, (3) recompute the battery power operation and HPP curtailment accounting for the charge and discharge efficiencies.

The implementation consist in estimated the reduction in charging power due to the different available generation and curtailment ($B_{LT}(t)$) as presented in equation 8, update the SOC ($E_{SOC-LT}(t)$) including the constraints of the new energy limits of the battery, equation 9, and finally recompute the battery power (P_{Bp}) to supply the SOC and curtailment ($P_{curt-LT}(t)$),
185   equation 10:

$$
\begin{aligned}
P_{loss}(t) &= \max(H(t) - H_{act}(t) - P_{curt}(t), 0) \\
B_{LT}(t) &= \min(B(t) + P_{loss}(t), 0) \qquad \text{if} \quad B(t) < 0 \\
B_{LT}(t) &\leq B_P \\
B_{LT}(t) &\geq -B_P
\end{aligned}
\tag{8}
$$

$$
\begin{aligned}
E_{SOC-LT}(t+1) &= \begin{cases} E_{SOC-LT}(t) - \eta_{charge} B_{LT}(t) \Delta t & \text{if} \quad B_{LT}(t) \leq 0 \\ E_{SOC-LT}(t) - B_{LT}(t) \Delta t / \eta_{discharge} & \text{if} \quad B_{LT}(t) \geq 0 \end{cases} \\
E_{SOC-LT}(t) &\geq B_E(t) \times [1 - B_{E\,depth}] \\
E_{SOC-LT}(t) &\leq B_E(t)
\end{aligned}
\tag{9}
$$

$$B_{LT}(t) = \begin{cases} (E_{SOC-LT}(t) - E_{SOC-LT}(t+1))/(\eta_{charge}\,\Delta t) & \text{if} \quad E_{SOC-LT}(t) - E_{SOC-LT}(t+1) \leq 0 \\ (E_{SOC-LT}(t) - E_{SOC-LT}(t+1))/(\Delta t/\eta_{discharge}) & \text{if} \quad E_{SOC-LT}(t) - E_{SOC-LT}(t+1) \geq 0 \end{cases}$$

$$P_{curt-LT}(t) = \max(H_{act}(t) + B_{LT}(t) - G, 0)$$
$$H_{LT}(t) = H_{act}(t) - P_{curt-LT}(t) + B_{LT}(t)$$

(10)

A comparison of the two versions of EMS is presented in Figure 7 for 500 different sizing capacities and levels of degradation
190 in 12 example locations (the 3 Indian example locations discussed in this article, and 3 locations in France, UK and Germany
each one of them using a time-varying Spot electricity price), a total of 6000 single year operations were run. It can be seen
that the rule-based EMS-LT correction is able to predict the revenue $(Pr(t)\,H(t))$ generated when the HPP is operating with
degradation. Even though there is bias in the relative error shown in a median of 1.4%, a 25% quantile of 0.4% and a 75%
quantile of 2.9%, most of the cases (within the 5% and 95% quantiles) have relative errors are between 0.0% and 5.8%.
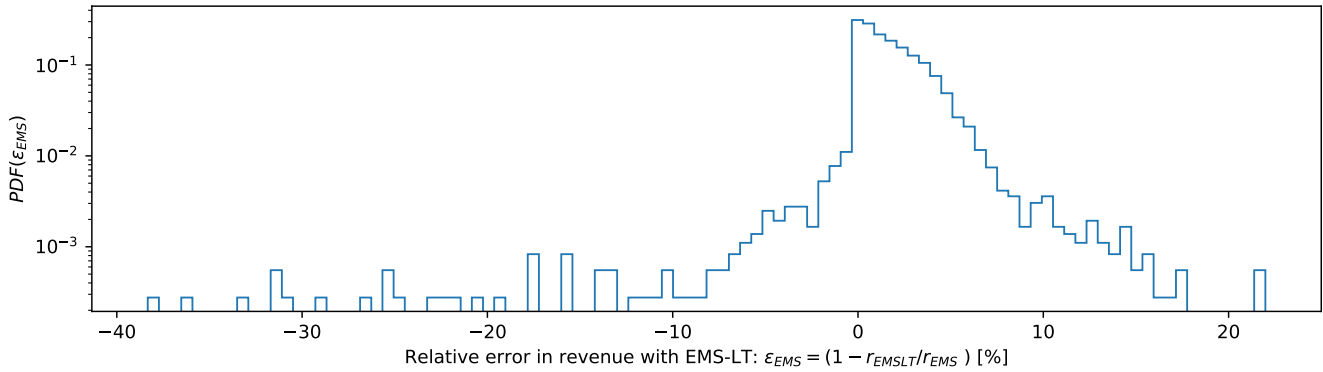
Figure 7. Cross-validation errors on rule.

195 **2.10 Wind plant costs model**

A simple WPP cost model consist in estimating the total capital expenditure costs (CAPEX, C_W) and operational and main-
tenance costs (OPEX, O_W) as a function of the installed capacity (given as number of turbines times the rated power of the
turbines: $W_{MW} = N_{wt}P_{rated}$), the cost of the turbines, their construction and civil infrastructure ($C_{WT} + C_{W\,civil}$). The OPEX
is divided into fix costs that scaled with the rated capacity of the plant ($O_{W\,fixed}$) and variable costs ($O_{W\,var}$) that scales with
200 the annual energy production of the wind turbines (AEP_W) and the ratio between the reference turbine and selected turbine
power rating. The wind turbine cost $f_{WT}(D, P_{rated}, hh)$ trend depends on the rotor diameter, the WT rated power and the
tower hub height and it is given by (Dykes et al., 2018). In order to have costs relative to a reference turbine, a user can provide

the cost and the characteristics of the reference turbine ($f_{WTref}(D_{ref}, P_{ratedref}, hh_{ref})$), from where the reference costs can be scaled, see equation 11.

$$
\begin{aligned}
C_W &= (f_{WT}/f_{WTref})(C_{WT} + C_{W\,civil})W_{MW} \\
O_W &= W_{MW}\,O_{W\,fixed} + AEP_W(P_{ratedref}/P_{rated})O_{W\,var}
\end{aligned}
\tag{11}
$$

2.11 PV plant costs model

A simple PV plant cost model consists in estimating the total capital expenditure costs (CAPEX, C_S) and operational and maintenance costs (OPEX, O_S) as a function of the installed capacity (S_{MW}), solar AC to DC ratio (r_{DC-AC}). The user provides PV cost per MW (DC) installation costs ($C_S + C_{S_{install}}$) and fixed operational costs (O_{Sfx}), while the inverter costs is provided per MW (AC) for a reference ratio of DC to AC (C_{invref}).

$$
\begin{aligned}
C_S &= (C_{PV} + C_{S_{install}})S_{MW}\,r_{DC-AC} + C_{invref}(r_{DC-ACref}/r_{DC-AC})S_{MW} \\
O_S &= O_{Sfx}\,S_{MW}\,r_{DC-AC}
\end{aligned}
\tag{12}
$$

2.12 Battery costs model

The battery plant cost model consists in estimating the total capital expenditure costs (CAPEX, C_B) and operational and maintenance costs (OPEX, O_B) as a function of the number of batteries required during the plant lifetime (N_b, assuming replacement of batteries after degradation) given the new battery energy (b_E) and power capacities (b_P). The CAPEX model splits the energy capacity costs (C_{bE}) and power capacity dependent costs which include power capacity, installation and control system costs ($C_{bP} + C_{bBOP} + C_{bcontrol}$). An equivalent number of present batteries (N_{Beq}) is used to reflect the decrease in costs of battery though out the lifetime of the battery given a battery price reduction per year (f_b) and the time of replacement of the i_b) battery in years ($y_b(i_b)$).

$$
\begin{aligned}
C_B &= N_{beq}(C_{bE}\,b_E) + (C_{bP} + C_{bBOP} + C_{bcontrol})b_P \\
O_B &= O_{bE}\,b_E \\
N_{Beq} &= \sum_{i_b=0}^{N_b-1}(1 - f_b)^{y_b(i_b)}
\end{aligned}
\tag{13}
$$

2.13 Electrical and shared infrastructure cost model (ele_cost)

A simple electrical infrastructure cost model consists in estimating the total capital expenditure costs (CAPEX, C_{el}) as a function of the grid capacity (G_{MW}), and balance of system costs and grid connection costs ($C_{BOS} + C_{grid}$) and land costs.

$$
\begin{aligned}
C_{el} &= (C_{BOS} + C_{grid})G_{MW} + C_{land}A_{HPP} \\
O_{el} &= 0
\end{aligned}
\tag{14}
$$

2.14 HPP financial model

A simple financial model consists in considering a different weighted average cost of capital (WACC) for wind, PV and battery. The WACC after tax ($WACC_{after_tax}$) then is the weighting sum of the WACCs for wind, PV, battery and electrical by their corresponding CAPEX, taking the mean WACC for the electrical costs shared across all technologies.

$$
\begin{aligned}
C_H &= C_W + C_S + C_b + C_{el} \\
O_H &= O_W + O_S + O_b + O_{el} \\
\text{WACC}_m &= (\text{WACC}_W + \text{WACC}_S + \text{WACC}_b)/3 \\
\text{WACC}_{tx} &= (C_W\,\text{WACC}_W + C_S\,\text{WACC}_S + \\
&\quad C_b\,\text{WACC}_b + C_{el}\,\text{WACC}_m)/C_H
\end{aligned}
\tag{15}
$$

The financial model then estimates the yearly incomes (I_y) and cashflow (F_y) as function of the average revenue over the year ($R_y = \langle Pr(t)\,H(t) - l \rangle_y$), the tax rate ($r_{tax}$) and WACC_{tx}. Net present value (NPV) and levelized costs of energy (LCoE) can then be calculated using the WACC_{tx} as the discount rate, as well as the internal rate of return (IRR).

$$
\begin{aligned}
I_y &= (R_y - O_H)(1 - r_{tax})(1 - \text{WACC}_{tx}) \\
F_y &= \begin{cases} -C_H & \text{for } y = 0 \\ I_y & \text{for } y > 0 \end{cases} \\[2ex]
NPV &= \sum_y F_y/(1 + \text{WACC}_{tx})^y \\[2ex]
0 &= \sum_y F_y/(1 + IRR)^y
\end{aligned}
\tag{16}
$$

$$
\begin{aligned}
C_L &= \sum_y (O_H/(1 + WACC_{tx})^y) + C_H \\
AEP_L &= \sum_y (AEP_y/(1 + WACC_{tx})^y) \\
LCoE &= C_L/AEP_L
\end{aligned}
$$

3 HPP sizing optimization

The HPP sizing optimization problem consists in minimizing LCoE or maximizing NPV over CAPEX by changing the design variables: rotor-tip to ground height clearance (h_c in [m]), turbine's specific power (sp in [m^2/MW]), turbine's rated power (p_{rated} in [MW]), number of wind turbines (N_{wt}), wind's installation density (ρ_W, in [MW/km^2]), solar capacity (S_{MW}), battery power capacity (b_P in [MW]) and battery energy storage capacity in hours at battery power capacity ($b_{E\,h}$). Furthermore, the sizing is forced to only take integer values of the design variables.

$$\min \quad y(x)$$

$$y(x) = \begin{cases} -NPV/C_H(x) \\ LCoE(x) \end{cases}$$

240

$$x = [h_c, sp, p_{rated}, N_{wt}, \rho_W, S_{MW}, \theta_{tilt}, \theta_{azim}, r_{DCAC}, B_P, B_{Eh}]$$ (17)

$$\text{s.t.} \quad D = 2\sqrt{P_{rated}/(\pi\, sp)}$$

$$hh = h_c + D/2$$

$$W_{MW} = N_{wt}\, p_{rated}$$

$$A_w = W_{MW}/\rho_W$$

$$B_E = B_{Eh}\, B_P$$

4 Surrogate based optimization

Surrogate-based optimization is used as the outer sizing optimization in order to reduce the number of full model evaluations during a gradient-based optimization (Jones et al., 1998). In this work, we use the Gaussian process (or Kriging) implementation from the Surrogate Modeling Toolbox (SMT) (Bouhlel et al., 2019). Modern Kriging surrogates with partial least squares

245 based training (KPLS) have been shown to be faster to train and evaluate because of the minimized number of meta-parameters obtained by applying dimensional reduction techniques such principal component analysis to the inputs (Bouhlel et al., 2016b). Furthermore, KPLS can be used to provide near optimal initial conditions in the training of standard Kriging (KPLSK) (Bouhlel et al., 2016a). KPLSK with squared exponential kernel and linear trend are used as a surrogate model over the design variables.

An updated version of the parallel efficient global optimization (Roux et al., 2020) is proposed in order to use a two-

250 step approach to (a) explore (find regions with candidates for global optimal) and (b) refine (propose model simulations that help the convergence of EGO optimization on local optima). See Algorithm 1. An initial database of model simulations is generated using Latin hyper-cube sampling (LHS) (McKay et al., 2000; Jin et al., 2003). Then in each optimization iteration, an exploration step identifies regions with candidates for global optimal based on the evaluation of the expected improvement of the surrogate. This is done by parallel execution over 10^4 random samples (per parallel process) in the design space. Then

255 the top-ranked (EI_x) points are clustered using Elkan's K-mean clustering algorithm (Elkan, 2003) and the best performing point per cluster is selected as a candidate (x_{EI}^+). A refinement step is performed around the current optimal perturbing of each dimension at a time (x_{opt}^+), depending on the iteration convergence the refinement focuses on local perturbations or evaluations of extremes per input dimension. Finally the model is evaluated in parallel ($y^+ \leftarrow \mathcal{M}(x^+)$). The surrogate $\hat{\mathcal{M}}$ is then updated with the updated list of model evaluations (x^+, y^+).

Algorithm 1 Parallel explore and refine EGO algorithm

$x = \text{LHS}(n_0)$

$y = \mathcal{M}(x)$ Initial simulation DB

$x_{opt} = \text{argmin}_x(y)$

while $i_{iter} < n_{max\,iter}$ **do**

   $\hat{\mathcal{M}} \leftarrow \text{train}(x, y)$ Train surrogate model

   $EI_x = \text{EI}(\hat{\mathcal{M}}, x_{opt}, x_x)$ **Explore** the expected improvement

   $x_{EI}^+ \leftarrow \text{get\_candidates}(x_x, EI_x)$ Get optimal candidates based on EI

   if $\epsilon \le \epsilon_{tol}$ **then**

     $x_{opt}^+ = \text{perturb\_around\_point}(x_{opt})$ **Refine** around current best

   else if $\epsilon > \epsilon_{tol}$ **then**

     $x_{opt}^+ = \text{extremes\_around\_point}(x_{opt})$ **Refine** on single variable extremes

   end if

   $x^+ = [x_{EI}^+, x_{opt}^+]$ Concatenate inputs for evaluation

   $y^+ = \mathcal{M}(x^+)$ Parallel model evaluation

   $x, y \leftarrow [x, x^+], [y, y^+]$ Update model evaluations

   $\epsilon = 1 - y_{opt}/\min(y)$ Update epsilon

   $x_{opt} = \text{argmin}_x(y)$ Update current optimal inputs

   $y_{opt} = \min(y)$ Update current optimal

end while

---

5 Results

A summary of assumptions costs and general specifications of HPP are presented in table 1. Two different scenarios for battery costs are presented on the example sites.

The detailed results of the hybrid plant sizing optimization based on LCoE or on NPV/C_H in three different locations in India are presented in tables 2 and 3, for the cheap battery and expensive battery scenarios correspondingly.

Table 2 shows that batteries are installed for NPV/C_H-based optimal sizing at the current costs of batteries (expensive batteries scenario), but the business case (IRR) for HPP with storage is marginal (0.08 or 0.07). In general, the optimizer tries to minimize the penalties by over-planting the generation or by introducing storage. On the *good solar* site, an HPP of Wind, PV and storage is obtained for the NPV/C_H-based design, while a single technology PV plant is obtained for the LCoE-based design. Note that the business case is negative for the LCoE-based design. On the *good wind* site a single wind plant with over-planting is selected for NPV/C_H-based design, while a single wind plant without over-planting is obtained for LCoE-based designs. The final size is a combination of reductions of land costs and wake losses, as it can be seen in the selection of larger spacing (ρ_W) for the LCoE-based design. It is interesting to see that both designs have very similar final LCoE values, which

	Expensive Batteries	Cheap Batteries
Grid [MW]	300	300
year_start	1995	1995
year_end	2019	2019
N_life	25	25
weeks_per_season_per_year	1	1
expected grid utilization (GU) at peak hours	42.5%	42.5%
wind_turbine_cost [Euro/MW]	851 000	851 000
wind_civil_works_cost [Euro/MW]	117 000	117 000
land_cost [Euro/km^2]	1.5	1.5
wind_fixed_onm_cost [Euro/MW /year]	12 800	12 800
d_ref [m]	100	100
hh_ref [m]	80	80
tracking	No	No
solar_PV_cost [Euro/MW]	219 000	219 000
solar_hardware_installation_cost [Euro/MW]	242 000	242 000
solar_fixed_onm_cost [Euro/MW]	8 150	8 150
pv_deg_per_year	0.005	0.005
battery_energy_cost [Euro/MWh]	180 000	90 000
battery_power_cost [Euro/MW]	64 000	32 000
battery_BOP_installation_commissioning_cost [Euro/MW]	73 000	36 000
battery_control_system_cost [Euro/MW]	18 000	9 000
battery_energy_onm_cost [Euro/MWh /year]	0	0
battery_lifetime [Full load cycles]	8 000	8 000
battery_depth_of_discharge	90%	90%
battery_min_E	70%	70%
battery_charge_efficiency	0.9	0.9
battery_price_reduction_per_year	0.05	0.05
hpp_BOS_soft_cost [Euro/MW]	120 000	120 000
hpp_grid_connection_cost [Euro/MW]	37 100	37 100
wind_WACC	0.052	0.052
solar_WACC	0.048	0.048
battery_WACC	0.08	0.08
discount_factor	0.06	0.06
tax_rate	0.22	0.22

Table 1. Assumptions for the HPP sizing optimization with two scenarios for battery costs.

highlights the fact that you can meet an LCoE target with multiple combinations of technologies. On the *bad solar and bad wind* site, a hybrid wind, PV and storage plant is selected for the NPV/C_H-based design with a marginally positive business

275 case. This illustrates why it is not possible to size HPP sites based on IRR, there are several configurations that will produce negative business cases and therefore have undefined IRR. Note that PV-only plants are in general over-planted (320 MW over 300 MW grid), the reason for this is to obtain a better annual energy production (AEP) and grid utilization factor (GUF).

Table 3 shows that hybrid plants only occur on NPV/C_H-based sizing optimization. This is in general an expected result from HPP sizing based on LCoE, as the optimizer will only select to install the technology that will provide the lowest LCoE.

280 NPV/C_H-based HPP designs include batteries in all locations in order to minimize the penalties except in the good wind site where it can meet the expected peak generation (and avoid penalty) just by over-planting the wind plant. In general, the lower costs of batteries produce better business cases on the NPV/C_H-based sites, in particular in the *bad solar and bad wind*. An example period of operation of the NPV/C_H-based sites is shown in figure 8.

Figure 8. Example of 10 days operation for NPV optimized HPPs (top) good solar site (bottom) good wind site. Cheap battery scenario.

Site	Good solar	Good solar	Good wind	Good wind	Bad solar & wind	Bad solar & wind
Design objective	LCoE	NPV/C_H	LCoE	NPV/C_H	LCoE	NPV/C_H
longitude	68.54	68.54	77.50	77.50	77.92	77.92
latitude	23.54	23.54	8.33	8.33	17.29	17.29
altitude	29.88	29.88	679.80	679.80	627.42	627.42
h_c [m]	10.0	10.0	10.0	10.0	13.0	10.0
sp [m2/W]	200.0	200.0	360.0	360.0	352.0	200.0
P_{rated} [MW]	1.0	1.0	4.0	4.0	1.0	1.0
N_{wt}	0.0	62.0	74.0	76.0	0.0	60.0
ρ_W [MW/km^2]	5.0	5.0	9.0	8.6	7.4	5.0
S_{MW}	329.0	400.0	0.0	0.0	335.0	400.0
θ_{tilt} [deg]	30.8	39.1	0.0	24.3	23.9	33.4
θ_{azim} [deg]	210.0	210.0	175.8	205.5	210.0	210.0
r_{DC-AC}	1.5	1.7	1.2	1.4	1.6	2.0
B_P [MW]	0.0	100.0	0.0	0.0	0.0	90.0
B_{Eh} [h]	1.0	2.0	9.0	3.0	9.0	4.0
C_{bfl}	10.9	0.0	1.6	1.9	10.9	0.4
Grid [MW]	300	300	300	300	300	300
Wind [MW]	0	62	296	304	0	60
Solar [MW]	329	400	0	0	335	400
Battery Power [MW]	0	100	0	0	0	90
Battery Energy [MWh]	0	200	0	0	0	360
Number_of_batteries	0	3	0	0	0	3
Rotor diam [m]	80	80	119	119	60	80
Hub height [m]	50	50	69	69	43	50
NPV/C_H	-0.26	0.26	1.52	1.52	-0.61	0.11
NPV [MEuro]	-41.01	79.90	414.05	423.61	-102.14	41.04
IRR	0.00	0.08	0.18	0.18	0.00	0.07
LCOE [Euro/MWh]	18.36	26.55	15.21	15.27	20.62	30.48
CAPEX [MEuro]	158.5	312.5	272.5	279.1	168.5	365.4
OPEX [MEuro]	2.2	5.3	6.7	6.9	2.5	5.6
Wind CAPEX [MEuro]	0.0	65.1	215.6	221.4	0.0	63.0
Wind OPEX [MEuro]	0.0	2.3	6.7	6.9	0.0	2.0
PV CAPEX [MEuro]	110.2	145.1	0.0	0.0	120.2	173.0
PV OPEX [MEuro]	2.2	3.0	0.0	0.0	2.5	3.6
Batt CAPEX [MEuro]	0.0	51.5	0.0	0.0	0.0	78.8
Batt OPEX [MEuro]	0.0	0.0	0.0	0.0	0.0	0.0
Shared CAPEX [MEuro]	48.3	50.8	57.0	57.7	48.3	50.7
Shared Opex [MEuro]	0.0	0.0	0.0	0.0	0.0	0.0
penalty lifetime [MEuro]	382.6	86.1	71.0	67.5	437.6	51.6
AEP [GWh]	737.4	1077.0	1759.0	1795.8	700.9	1088.7
GUF	0.28	0.41	0.67	0.68	0.27	0.41
Total curtailment [GWh]	190	2506	0	335	233	1330
opt time [min]	14	15	9	12	8	15

Table 2. HPP Sizing optimization results in the example sites with respect NPV/C_H and LCoE for expensive batteries scenario.

Site	Good solar	Good solar	Good wind	Good wind	Bad solar & wind	Bad solar & wind
Design objective	LCoE	NPV/C_H	LCoE	NPV/C_H	LCoE	NPV/C_H
longitude	68.54	68.54	77.50	77.50	77.92	77.92
latitude	23.54	23.54	8.33	8.33	17.29	17.29
altitude	29.88	29.88	679.80	679.80	627.42	627.42
h_c [m]	10.0	10.0	10.0	10.0	13.0	10.0
sp [m2/W]	200.0	200.0	360.0	360.0	352.0	200.0
P_{rated} [MW]	1.0	1.0	4.0	4.0	1.0	1.0
N_{wt}	0.0	41.0	74.0	74.0	0.0	26.0
ρ_W [MW/km^2]	5.8	5.0	9.0	8.2	7.4	5.0
S_{MW}	335.0	400.0	0.0	0.0	335.0	400.0
θ_{tilt} [deg]	28.9	35.2	0.0	0.0	23.9	24.7
θ_{azim} [deg]	210.0	210.0	175.8	187.8	210.0	210.0
r_{DC-AC}	1.5	1.7	1.2	1.2	1.6	2.0
B_P [MW]	0.0	100.0	0.0	0.0	0.0	100.0
B_{Eh} [h]	9.0	4.0	9.0	9.0	9.0	6.0
C_{bfl}	10.9	0.0	1.6	1.6	10.9	0.0
Grid [MW]	300	300	300	300	300	300
Wind [MW]	0	41	296	296	0	26
Solar [MW]	335	400	0	0	335	400
Battery Power [MW]	0	100	0	0	0	100
Battery Energy [MWh]	0	400	0	0	0	600
Number_of_batteries	0	3	0	0	0	3
Rotor diam [m]	80	80	119	119	60	80
Hub height [m]	50	50	69	69	43	50
NPV/C_H	-0.23	0.48	1.52	1.52	-0.61	0.31
NPV [MEuro]	-37.51	137.30	414.05	415.66	-102.14	95.96
IRR	0.00	0.10	0.18	0.18	0.00	0.09
LCOE [Euro/MWh]	18.37	24.13	15.21	15.21	20.62	26.90
CAPEX [MEuro]	161.8	284.1	272.5	273.5	168.5	310.7
OPEX [MEuro]	2.3	4.6	6.7	6.7	2.5	4.5
Wind CAPEX [MEuro]	0.0	43.0	215.6	215.6	0.0	27.3
Wind OPEX [MEuro]	0.0	1.5	6.7	6.7	0.0	0.9
PV CAPEX [MEuro]	113.5	147.8	0.0	0.0	120.2	173.0
PV OPEX [MEuro]	2.3	3.0	0.0	0.0	2.5	3.6
Batt CAPEX [MEuro]	0.0	43.7	0.0	0.0	0.0	61.7
Batt OPEX [MEuro]	0.0	0.0	0.0	0.0	0.0	0.0
Shared CAPEX [MEuro]	48.3	49.6	57.0	57.9	48.3	48.7
Shared Opex [MEuro]	0.0	0.0	0.0	0.0	0.0	0.0
penalty lifetime [MEuro]	379.4	58.3	71.0	69.9	437.6	42.3
AEP [GWh]	754.2	1061.1	1759.0	1764.3	700.9	1029.2
GUF	0.29	0.40	0.67	0.67	0.27	0.39
Total curtailment [GWh]	297	1375	0	0	233	376
opt time [min]	12	15	7	9	8	15

Table 3. HPP Sizing optimization results in the example sites with respect NPV/C_H and LCoE for cheap batteries scenario.

6 Conclusions

285 NPV-over-CAPEX optimal hybrid power plants are obtained across India in order to mitigate the penalties of not reaching the expected energy generation at peak hours. Li-ion batteries are installed on sites that can not mitigate penalties by over-planting. the results show how changing from LCoE to NPV/C_H-based design allows the optimizer to over-plant the HPP to maximize the revenue by balancing the CAPEX, OPEX and power curtailment coming from the oversized design.

Battery degradation plays an important role in HPP sizing as the additional costs of replacing the battery two over three
290 times will change the financial viability of the project. For this reason, future work will look into integrating constraints of the amount of battery load cycles or battery lifetime consumption within the EMS optimization.

Code and data availability. HyDesign is an open source code for design and control of utility scale wind-solar-storage based hybrid power plant (HPP). The documentation and example interactive examples are available at(https://topfarm.pages.windenergy.dtu.dk/hydesign/); the input data including weather and price signals for the example Indian sites used in this article are available in the HyDesign repository under
295 examples (https://gitlab.windenergy.dtu.dk/TOPFARM/hydesign).

Author contributions. JPM is responsible for the model development, overall implementation and the article. HH implemented the rule-based correction method. MFM contributed to the implementation of the parallel EGO algorithm. MG contributed in the improvement of the EMS formulation. RZ contributed with the initial implementation of battery degradation model. KD provided funding and supervision. All authors contributed to the article.

300 *Competing interests.* The authors declare that there are no competing interests.

Acknowledgements. Part of the research was performed in REALISE project funded by EUDP (journal number - 64021-2049) and as part of the Indo-Danish project "HYBRIDize" (https://orbit.dtu.dk/en/projects/optimized-design-and-operation-of-hybrid-power-plant) funded by Danish Innovationsfonden (IFD). KD would also like to acknowledge EUDP IEA Wind Task 50 project for supporting his hours for contributing to the article.

References

Al-Lawati, R. A., Crespo-Vazquez, J. L., Faiz, T. I., Fang, X., and Noor-E-Alam, M.: Two-stage stochastic optimization frameworks to aid in decision-making under uncertainty for variable resource generators participating in a sequential energy market, Applied Energy, 292, 116 882, 2021.

Bouhlel, M. A., Bartoli, N., Otsmane, A., and Morlier, J.: An improved approach for estimating the hyperparameters of the kriging model for high-dimensional problems through the partial least squares method, Mathematical Problems in Engineering, 2016, 2016a.

Bouhlel, M. A., Bartoli, N., Otsmane, A., and Morlier, J.: Improving kriging surrogates of high-dimensional design models by Partial Least Squares dimension reduction, Structural and Multidisciplinary Optimization, 53, 935–952, 2016b.

Bouhlel, M. A., Hwang, J. T., Bartoli, N., Lafage, R., Morlier, J., and Martins, J. R. R. A.: A Python surrogate modeling framework with derivatives, Advances in Engineering Software, p. 102662, https://doi.org/https://doi.org/10.1016/j.advengsoft.2019.03.005, 2019.

Camargo, L. R. and Schmidt, J.: Simulation of multi-annual time series of solar photovoltaic power: Is the ERA5-land reanalysis the next big step?, Sustainable Energy Technologies and Assessments, 42, 100 829, 2020.

Commission, I.-I. E. et al.: IEC 61400-1, Wind turbines – Part 1: Design requirements., 2017.

Das, K., Grapperon, A. L. T. P., Sørensen, P. E., and Hansen, A. D.: Optimal battery operation for revenue maximization of wind-storage hybrid power plant, Electric Power Systems Research, 189, 106 631, 2020.

Davies, J. and Hay, J.: Calculation of the Solar Radiation Incident on an Inclined Surface in Proc, in: First Canadian Solar Radiation Data Workshop (JE Hay and TK Won, eds.), pp. 32–58, 1978.

Downing, S. D. and Socie, D.: Simple rainflow counting algorithms, International journal of fatigue, 4, 31–40, 1982.

Dykes, K., King, J., DiOrio, N., King, R., Gevorgian, V., Corbus, D., Blair, N., Anderson, K., Stark, G., Turchi, C., and Moriarty, P.: Opportunities for Research and Development of Hybrid Power Plants, https://doi.org/10.2172/1659803, 2020.

Dykes, K. L., Damiani, R. R., Graf, P. A., Scott, G. N., King, R. N., Guo, Y., Quick, J., Sethuraman, L., Veers, P. S., and Ning, A.: Wind turbine optimization with WISDEM, Tech. rep., National Renewable Energy Lab.(NREL), Golden, CO (United States), 2018.

Elkan, C.: Using the triangle inequality to accelerate k-means, in: Proceedings of the 20th international conference on Machine Learning (ICML-03), pp. 147–153, 2003.

Gorman, W., Mills, A., Bolinger, M., Wiser, R., Singhal, N. G., Ela, E., and O'Shaughnessy, E.: Motivations and options for deploying hybrid generator-plus-battery projects within the bulk power system, The Electricity Journal, 33, 106 739, 2020.

Hersbach, H., Bell, B., Berrisford, P., Hirahara, S., Horányi, A., Muñoz-Sabater, J., Nicolas, J., Peubey, C., Radu, R., Schepers, D., et al.: The ERA5 global reanalysis, Quarterly Journal of the Royal Meteorological Society, 2020.

Holmgren, W. F., Hansen, C. W., and Mikofski, M. A.: pvlib python: a python package for modeling solar energy systems, Journal of Open Source Software, 3, 884, https://doi.org/10.21105/joss.00884, 2018.

Jin, R., Chen, W., and Sudjianto, A.: An efficient algorithm for constructing optimal design of computer experiments, in: International Design Engineering Technical Conferences and Computers and Information in Engineering Conference, vol. 37009, pp. 545–554, 2003.

Jones, D. R., Schonlau, M., and Welch, W. J.: Efficient global optimization of expensive black-box functions, Journal of Global optimization, 13, 455–492, 1998.

Jordan, D. C., Deceglie, M. G., and Kurtz, S. R.: PV degradation methodology comparison—A basis for a standard, in: 2016 IEEE 43rd Photovoltaic Specialists Conference (PVSC), pp. 0273–0278, IEEE, 2016.

Kasten, F. and Young, A. T.: Revised optical air mass tables and approximation formula, Applied optics, 28, 4735–4738, 1989.

Khaloie, H., Anvari-Moghaddam, A., Contreras, J., and Siano, P.: Risk-involved optimal operating strategy of a hybrid power generation company: A mixed interval-CVaR model, Energy, 232, 120 975, 2021a.

Khaloie, H., Anvari-Moghaddam, A., Hatziargyriou, N., and Contreras, J.: Risk-constrained self-scheduling of a hybrid power plant consid-
345   ering interval-based intraday demand response exchange market prices, Journal of Cleaner Production, 282, 125 344, 2021b.

King, D. L., Kratochvil, J. A., and Boyson, W. E.: Photovoltaic array performance model, United States. Department of Energy, 2004.

King, D. L., Gonzalez, S., Galbraith, G. M., and Boyson, W. E.: Performance model for grid-connected photovoltaic inverters., Tech. rep.,
Sandia National Laboratories, 2007.

Maxwell, E. L.: A quasi-physical model for converting hourly global horizontal to direct normal insolation. Technical Report No. SERI/TR-
350   215-3087., Solar Energy Research Institute, 1987.

McKay, M. D., Beckman, R. J., and Conover, W. J.: A comparison of three methods for selecting values of input variables in the analysis of
output from a computer code, Technometrics, 42, 55–61, 2000.

Murcia, J. P., Koivisto, M. J., Luzia, G., Olsen, B. T., Hahmann, A. N., Sørensen, P. E., and Als, M.: Validation of European-scale simulated
wind speed and wind generation time series, Applied Energy, 305, 117 794, 2022.

355   Pedersen, M. M., Meyer Forsting, A., van der Laan, P., Riva, R., Alcayaga Román, L. A., Criado Risco, J., Friis-Møller, M., Quick, J.,
Schøler Christiansen, J. P., Valotta Rodrigues, R., Olsen, B. T., and Réthoré, P.-E.: PyWake 2.5.0: An open-source wind farm simulation
tool, https://gitlab.windenergy.dtu.dk/TOPFARM/PyWake, 2023.

Roux, É., Tillier, Y., Kraria, S., and Bouchard, P.-O.: An efficient parallel global optimization strategy based on Kriging properties suitable
for material parameters identification, Archive of Mechanical Engineering, 67, 2020.

360   Safari, M., Morcrette, M., Teyssot, A., and Delacourt, C.: Multimodal physics-based aging model for life prediction of Li-ion batteries,
Journal of The Electrochemical Society, 156, A145, 2008.

Shi, Y., Xu, B., Tan, Y., and Zhang, B.: A convex cycle-based degradation model for battery energy storage planning and operation, in: 2018
Annual American Control Conference (ACC), pp. 4590–4596, IEEE, 2018.

Tripp, C., Guittet, D., King, J., and Barker, A.: A simplified, efficient approach to hybrid wind and solar plant site optimization, Wind Energy
365   Science, 7, 697–713, https://doi.org/10.5194/wes-7-697-2022, 2022.

Vetter, J., Novák, P., Wagner, M. R., Veit, C., Möller, K.-C., Besenhard, J., Winter, M., Wohlfahrt-Mehrens, M., Vogler, C., and Hammouche,
A.: Ageing mechanisms in lithium-ion batteries, Journal of power sources, 147, 269–281, 2005.

Wang, Y., Zhao, H., and Li, P.: Optimal offering and operating strategies for Wind-Storage system participating in spot electricity markets
with progressive stochastic-robust hybrid optimization model series, Mathematical Problems in Engineering, 2019, 2019.

370   Xu, B., Oudalov, A., Ulbig, A., Andersson, G., and Kirschen, D. S.: Modeling of lithium-ion battery degradation for cell life assessment,
IEEE Transactions on Smart Grid, 9, 1131–1140, 2016.

Zong, H. and Porté-Agel, F.: A momentum-conserving wake superposition method for wind farm power prediction, Journal of Fluid Me-
chanics, 889, https://doi.org/10.1017/jfm.2020.77, 2020.